NASA CR-66010

DEVELOPMENT OF A SECOND GENERATION PROTOTYPE REFLECTOMETER FOR REFLECTANCE MEASUREMENT IN SPACE

By Arthur A. Olsen
Peter A. Button
Donald H. McClelland

Prepared under Contract No. NAS1-4660 by
ELECTRO-OPTICAL SYSTEMS, INC.
A Subsidiary of Xerox Corporation
Pasadena, California

for

NATIONAL AERONAUTICS AND SPACE ADMINISTRATION

CONTENTS

ILLUSTRATIONS

DEVELOPMENT OF A SECOND GENERATION PROTOTYPE REFLECTOMETER FOR REFLECTANCE MEASUREMENT IN SPACE

By Arthur A. Olsen
Peter A. Button
Donald H. McClelland

SUMMARY

A full-scale prototype rotating arm reflectometer has been designed, built, and tested. In the design of this prototype, several optical problems were considered which had proved troublesome in a previous optical model. While this prototype was not meant to be a flightworthy instrument, attention was paid in the design to the desirability of minimizing volume, weight, and instrument power requirements.

The prototype instrument has an overall diameter of 50.8 cm, an overall height of 23.4 cm, and a weight of approximately 13 kg. It serially measures the specular reflectance of a number of reflective surface samples which are mounted on the prototype. Measurement is made both of overall reflectance and of reflectance in four individual spectral bands.

Control and power circuitry are mounted remotely in a control box attached to the prototype by a cable.

Six measurement channels are provided. One uses an integral tungsten lamp as a source, and the other five channels use energy from the sun. Of the solar channels, one measures the total reflected energy, while the other four make spectral measurements in the bands 0.3 - 0.45μ, 0.45 - 0.65μ, 0.65 - 1.2μ, and 1.2 - 2.0μ.

In the prototype, nine sample positions are provided, spaced on a radius of 23 cm. Two of the nine sample positions are occupied by reference samples. One is a "0%" sample, and the other is a highly stable reflective prism of fused quartz.

Internally, the optical beams of the reflectometer are chopped at a frequency of 105 cps by a tuning fork chopper. Detection is by lead sulphide detectors, followed by amplification and signal processing circuitry which gives a dc output in each channel which is proportional to the reflectance of the sample being scanned.

The arm is gear driven by a dc gearhead motor. Nominal arm rotation speed is about 3 rpm.

While the prototype instrument was in general satisfactory during tests, two main optical problems were encountered. The first is that the prototype is not completely insensitive to curvature of the reflective sample. Change from a flat sample to one of 2.54 meter focal length changed the indicated reflectance by 14 percent and 21 percent in two channels tested. The other sizeable problem was cross talk into the 0.3 - 0.45μ spectral channel. Almost all of the solar energy in this band is filtered out by the earth's atmosphere, hence this channel of the prototype was made very sensitive, and even the small amount of light scattered from the other channels is troublesome. The greatly increased amount of solar energy in the 0.3 - 0.45μ band above the earth's atmosphere would obviate this problem in a flightworthy instrument.

A fixture was built for pressure testing and vacuum testing the rotating seal which would be necessary on the arm of a flightworthy reflectometer. Seals were designed and fabricated using a commercially-available polyurethane material. Friction level and leakage tests of these seals were performed, some in a high vacuum. Performance of the seals was uneven; one of the seals was satisfactory, giving low friction levels and essentially no leakage in a high-vacuum test, while other seals soon failed, giving high leakage and friction levels.

Tests were run to determine the attitude control accuracy required in the solar channels of the reflectometer prototype. Satisfactory signal levels could be obtained over a total range of about 6 degrees (0.10 radian) of motion in one axis, and 8 degrees (0.14 radian) in the other. While output level was not constant with these motions, it could be corrected for by knowing the actual direction of the sun.

INTRODUCTION

This is the final technical report covering the work accomplished by Electro-Optical Systems, Inc. on Contract NAS 1-4660 with the NASA, Langley Research Center for the design, development, and fabrication of a second-generation prototype reflectometer for a space experiment for reflective surface samples.

The development of space power systems for advanced space missions will be one of the most critical problem areas in space technology during the next one or two decades. The only two basic energy sources which presently appear capable of meeting the requirements of these missions are solar energy and nuclear energy. Up to certain power levels, solar energy systems are lighter, safer to operate, and less expensive. A solar energy system consists of the solar cencentrator, the absorber, and the energy conversion device. The overall system performance is a function of the performance of these three subsystems.

The performance of a solar concentrator is dependent on the geometrical accuracy and the reflectance of the concentrator surface. Considerable effort has been and is being directed toward developing fabrication techniques for obtaining the required geometrical accuracies and in investigating materials which, in ground tests, demonstrate high reflectance. One area in which data are critically weak, however, is that of performance and life of highly reflective surfaces in the space environment. This results from two factors: uncertainty of the space environment and the difficulty of simulating effectively the characteristics of the space environment which are known. The problems of simulation are made particularly difficult by the necessity of combining different kinds of physical stresses and continuing the requisite tests for long durations.

Data on the behavior of reflective surfaces in the space environment are also needed for other applications such as space vehicle temperature control. Further, it is expected that the change in reflectance characteristics of specular surfaces will provide information about the space environment which is not obtainable from present instrumentation.

The present contract is the third between Electro-Optical Systems, Inc. and NASA, Langley Research Center in the field of reflectometry in space. The first contract was a study program to define a flight

experiment for determining the effects of the space environment of the performance of solar concentrator reflective surfaces (NASA CR-55893). This program included identification of the factors in space that will effect concentrator surfaces, the selection of concentrator surface samples for evaluation, and the analysis and prediction of the effects of various space environmental factors on concentrator surfaces. The program included consideration of the simulation of the space environment in ground tests. The main portion of the program comprised of the design of two complete satellite systems for testing concentrator surfaces in space, including the consideration of launch vehicles, orbits, onboard power, telemetry, command system, and attitude control. The basic concept of the rotating arm reflectometer originated on this program. A follow-on program included the design and fabrication of a breadboard prototype model of the reflectometer system, an analytical study of bearings and seals in the space environment, a study of valving for attitude control, and a study of methods for separation of effects (NASA CR-60400). The reflectometer breadboard built under this program demonstrated the basic validity of the rotating-arm reflectometer approach. The other three task items also demonstrated the validity of the flight experiment approach conceived in the previous program.

The purpose of the present reflectometer program is the design, fabrication, and testing of a prototype of an improved reflectometer instrument. A further objective of this program has been the fabrication and testing of a rotating seal which could be used for the hub of a flight-worthy reflectometer instrument.

PROTOTYPE REFLECTOMETER

Philosophy and Objectives

The overall objective of the present program was to advance the state of the art of reflectometer instrumentation to a point where the development of flight-worthy hardware could be started. The basic rotating arm reflectometer concept had been shown to be sound. In this type of instrument, a number of small reflective samples are arranged face up on the periphery of a disc, where in a flight-worthy instrument they would be exposed to the space environment. An arm, which is pivoted at the center of the disc, rotates above the samples, scanning each one in turn. The arm projects a beam of light onto the sample being tested and receives the reflected portion of the light. The reflected light passes down into the body of the reflectometer below the disc, where there are further processing optics and the detectors and electronic signal processing necessary to analyze the light reflected. A single instrument, thus, serially measures the reflectance of a number of samples. While the implementation of the concept is not so simple as its description, the basic instrument is simple and sturdy, and offers a comparatively quick, precise, positive way of measuring and comparing the reflectance of many different kinds of specular surfaces.

Reflectance of each sample is measured simultaneously by two separate systems. One system uses a tungsten lamp as the light source, and the other uses energy from the sun which is admitted to the reflectometer through a window near the center of the disc. This system measures not only the total specular reflectance of the sample but also analyzes the reflectance in four spectral bands.

In the design of the present prototype (Fig. 1), considerable attention was paid to problem areas which had been encountered in the design and construction of the previous prototype. In particular, the first model was subject to ambiguities in the measurement of spectral reflectance if the orientation of the reflectometer relative to the sun changed. Further, the measurements made with the first model were sensitive to slight sample curvature and misalignment.

The second prototype has been designed to minimize the effect of attitude errors and sample curvature and misalignment, while still producing satisfactory signal levels and measurement precision. The design has also largely eliminated stray light problems which had troubled the previous optical model. While recognizing that this prototype is not a flight-worthy model, and the ruggedness and extreme light weight which might be necessary in a flight-worthy model were not necessary here,

considerable attention was paid in the design to instrument weight, packaging, and power requirements. As a result the present instrument has power requirements, weight, and volume which are minimal for such a prototype. The prototype has an overall diameter of 50.8 cm, an overall height of 23.4 cm and a weight of approximately 13 Kg.

Considerable effort was spent on a revised optical design for the prototype. While the basic concept of obtaining some redundancy by using two reflectometer systems in parallel was retained, sufficient optical details were changed to warrant calling this a new design. The objective was to attain an optical design satisfactory for use in a flight-worthy instrument with only very minor changes. These changes might include additional mirrors whose only purpose is to fold the optical paths for more convenient packaging, should there be unusual packaging requirements on the satellite picked to carry this instrument.

Alternately, path-folding mirrors which are used in the prototype could be omitted in a flight-worthy instrument. Further, the size of the instrument could be changed by scaling it up or down and including more or fewer samples depending on the available surface area and volume. The prototype is of a size large enough for fairly easy fabrication, and small enough for convenient handling as a demonstration model. The mechanical packaging of the instrument is intended to be sufficiently rugged to permit shipping and handling, but not to be flight-worthy. Similarly, the electronics are similar in concept to those which would be used on a flight-worthy model, but are not miniaturized, ruggedized, or meant to be stable under extreme environmental conditions.

Considerable uncertainty existed concerning the seal necessary to permit the interior of the reflectometer to be pressurized and still allow the arm to rotate periodically. Since this kind of a seal would not be necessary for an earth-bound prototype, it was decided to divorce the seal from the construction of the actual prototype, and build a seal test fixture suitable for testing a variety of seals independently of the prototype reflectometer. As a result, the prototype is not capable of pressurization as would be a flight-worthy instrument.

Amplification of the electronic signals in the earlier optical model had been by dc amplifiers. In order to obviate the drift and noise problems associated with dc processing, it was decided to use some scheme for chopping the optical beams in the present prototype, then use ac amplification and subsequent demodulation.

On the earlier optical model, the control and basic power circuitry had been mounted within the model itself. In order to better simulate the weight and volume requirements of a flight-worthy instrument, the power and control circuitry are mounted in a control box (see Figure 2) attached to the instrument by a cable 3 meters long.

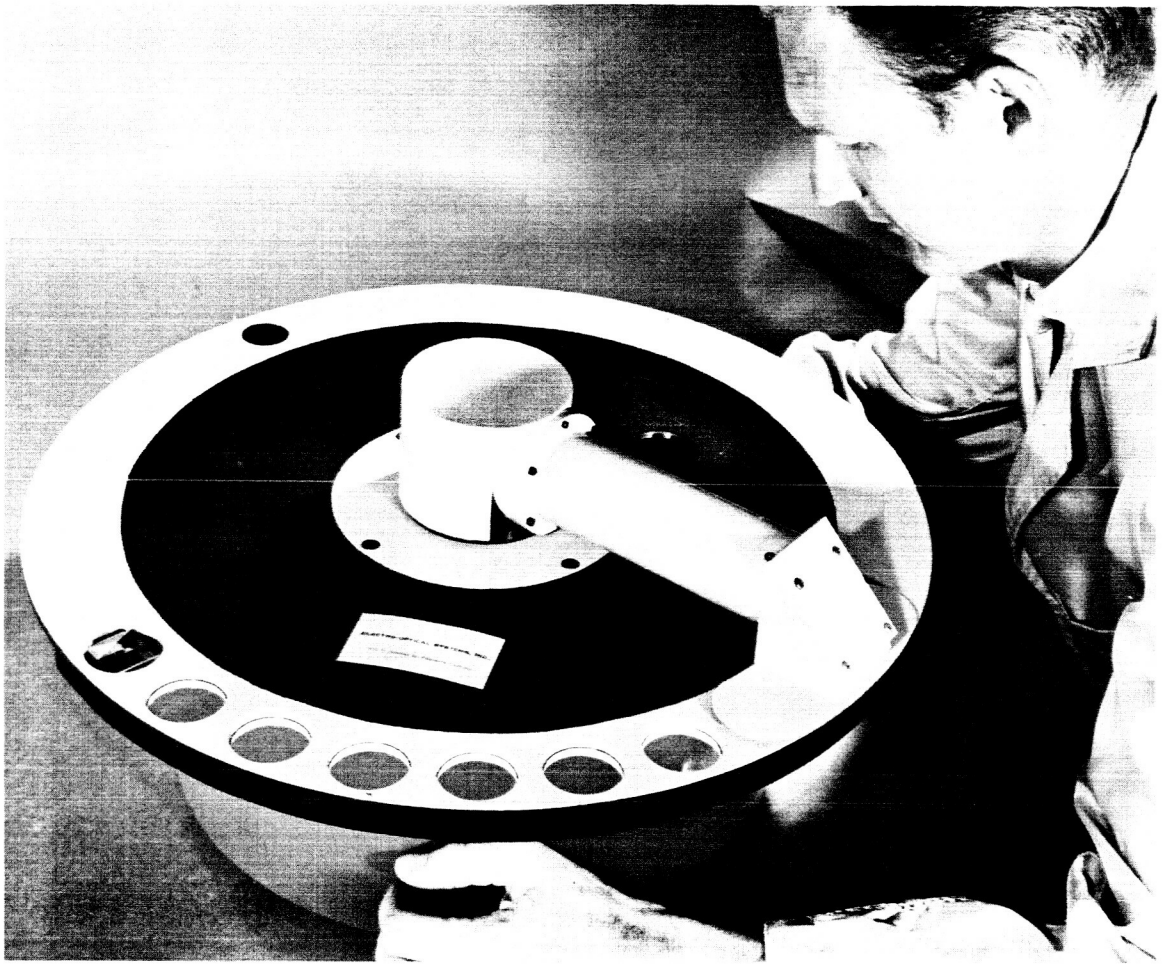

FIGURE 1 PROTOTYPE REFLECTOMETER

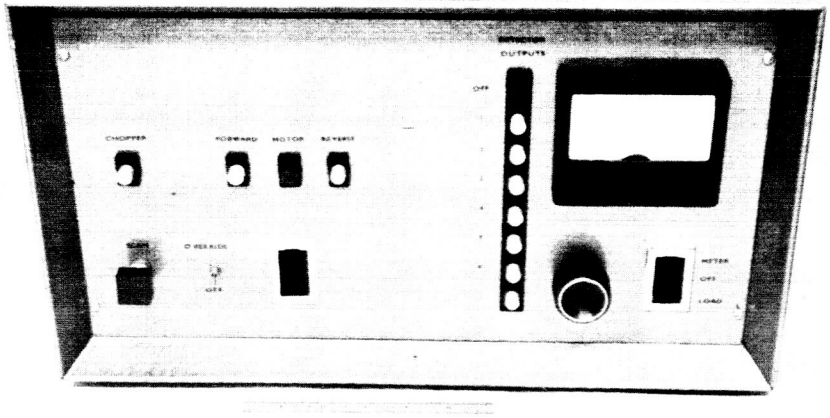

FIGURE 2 REFLECTOMETER CONTROL BOX

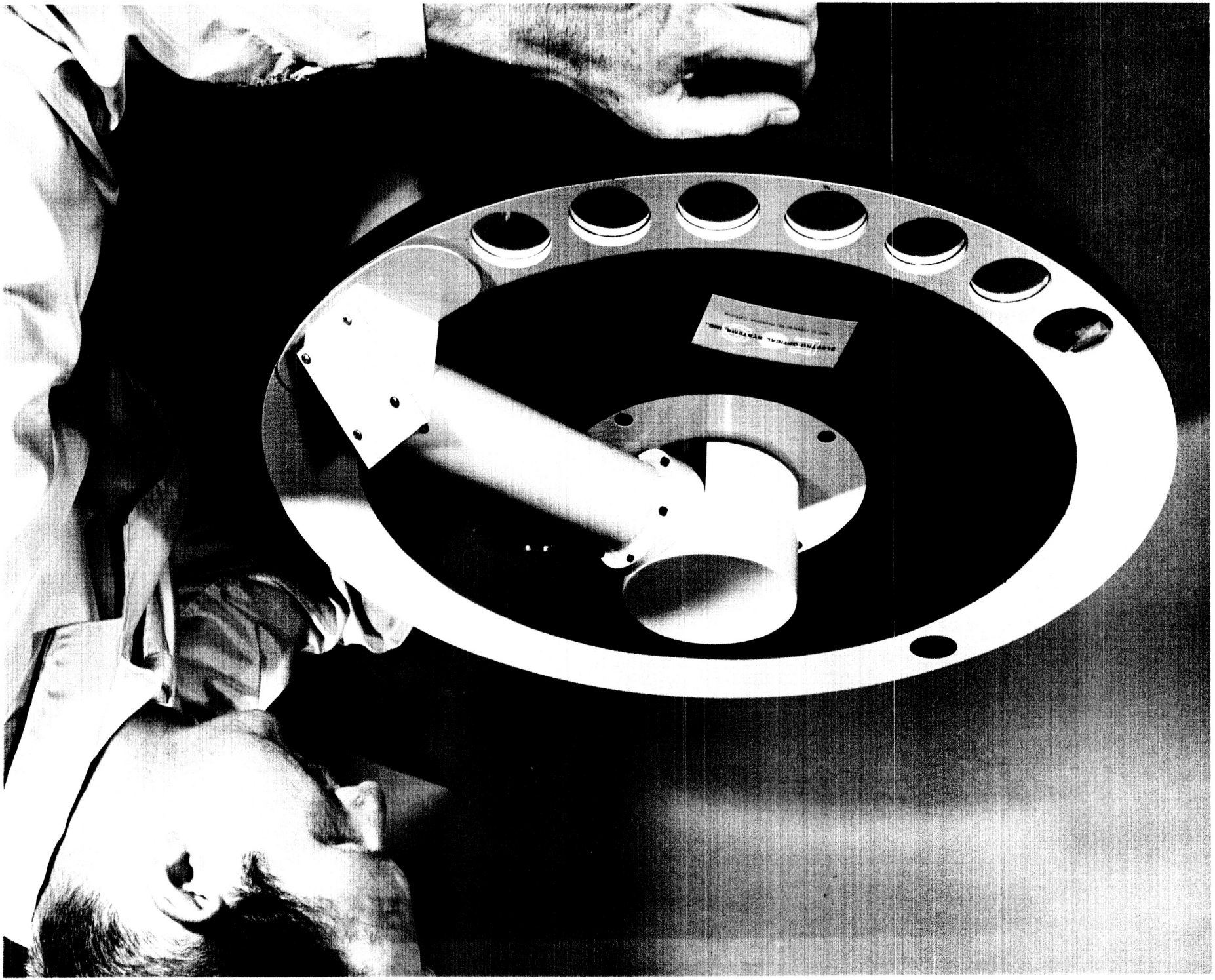

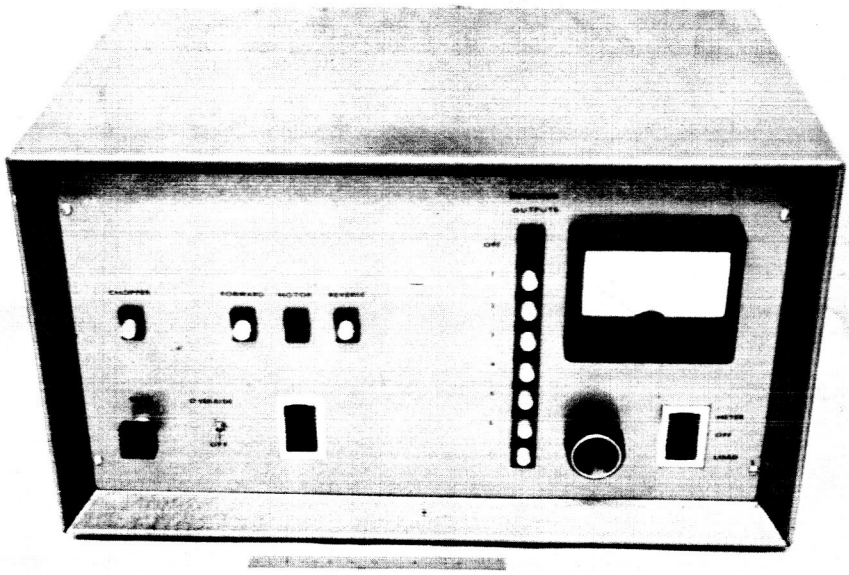
OUTPUTS
CHOPPER
FORWARD
MOTOR
REVERSE

Optical Design

Basic considerations. – The basic components of a reflectometer are a radiation source, a reflective sample, and a detector for the reflected radiation. A choice of source and detector must be made considering a number of factors. Among these are the spectral band to be considered, the sensitivity necessary, the desired speed of response, and the available space, weight, and power.

If the geometry is such that the detector picks up only the radiation which bounces from the sample surface considered as a mirror, the measurement made is called specular reflectance. If, on the other hand, the geometry permits the detector to pick up all of the radiation which is reflected from the sample, regardless of the angle, then the measurement is of diffuse reflectance. For the present purpose, only specular reflectance is of interest.

Since in general the amount of radiation impinging on the detector is a function not only of the specular reflectivity of the sample but also of the source-sample-detector geometry, provision must be made for calibration of the system, ordinarily by substitution of a sample of known reflectivity. This can be done, of course, either by moving the reflectometer from sample to sample or by substituting samples in a stationary reflectometer. In the present case, the sample and most of the optics of the reflectometer are stationary and the impinging and reflected beams are carried to the samples by a moving arm.

Two different sources are used in the prototype reflectometer, one a tungsten lamp, the other an image of the sun. This provides a measure of redundancy and thus increased reliability. The reflected energy in the solar channel is to be separated into a number of different spectral bands for spectrometric measurements. It is further necessary that the optical arrangement in both systems be such as to permit use of an optical chopper.

Basic system. –A basic objection to the primitive system, described above, is that it is relatively inefficient. Addition of a lens to focus the beam leaving the source permits much more energy to impinge upon the reflective sample and thus permits a higher signal level at the detector. Effectively, this lens forms an image of the source at the detector as seen "through" the reflective sample. Geometry in this kind of a system is still critical, since non-uniformities in the source are compounded with non-uniformities across the surface of the detector, and what might appear negligible changes in sample orientation can produce radical changes in signal level at the detector. Furthermore, if the sample is not absolutely flat, the image of the source is no longer formed accurately at the surface of the detector and the signal level at the detector can again change radically.

To alleviate these problems, the image of the source can be formed at a field lens instead of at the detector. This kind of basic system is illustrated in Figure 3. Here there is an image at the detector, but the image is of the objective lens, and not of the source. This objective lens image is quite uniform, even though the source may be markedly uneven. The effect of sample curvature, seen at the center of the sample, (see Figure 4), is to place a weak lens at the plane of the sample. This has the effect of moving the objective lens image out of the plane of the detector, thus changing the irradiance somewhat at the detector. Off the center of the sample, the beam is not only defocused but tilted slightly. This is the same effect that would be caused by angular misalignment even with a perfectly flat sample. This has the effect of moving the objective lens image somewhat at the detector, but so long as the detector stays completely within the image of the objective lens, the change in irradiance seen by the detector is slight.

In the tungsten lamp channel, the source is, of course, stationary. In the solar channels, however, the source is an image of the sun, and motion of the instrument relative to the sun changes the position of the image within the reflectometer. As seen in Figure 3, this has the effect of changing the position of the source image within the field lens, but causes no radical changes in irradiance at the detector so long as the solar re-image stays completely within the field lens.

At this point, source and detector size and configuration remain to be fixed. These interact with the geometric parameters of the basic two-lens system, such as focal length, lens diameter, and lens to lens spacing. It is assumed here that the sample is centered between the two lenses. The problem is simplest in the case of the tungsten channel, where it is merely a matter of picking a tungsten lamp with a small filament. Some work was done in fabricating an array of ultra-miniature 6-volt lamps, but this was discontinued when these lamps were found to be excessively subject to damage during soldering. Further, these lamps would have required either use of a power-wasting dropping resistor to reduce the 24 volts assumed available from the power supply to the 6 volts necessary for the lamps, or else the use of four lamps in the series to make the required 24 volts. Schemes were considered to increase the reliability of the tungsten source which included the use of two conventional bulbs operating through a beamsplitter, as well as use of a spatially interlocked array of electrically separate lamps. The final decision was to use a special type 327 lamp as the source. This 28-volt bulb is conventionally used in aircraft instrument lighting applications, and a 25,000-hour life version of it commercially available. The filament is very small, a "u" shaped configuration of about 2.5 mm on a side. In the prototype, this bulb is used at 20 volts which is produced by a small resistor - zener diode regulator.

Assuming that conventional reliability extrapolations are correct and that the wear-out or burn-out mechanism is not changed by operating at reduced voltage, the rated life of this bulb at 20 volts should be on the order of a million hours. This should not be the weak link in the system!

In the solar channel, an image of the sun must be used as a source. The image forming function is combined with one path-folding mirror by using a spherical concave mirror 45° (0.78 radian) from its optical axis. Use this far off the axis produces considerable astigmatism in the image, but since the solar image is re-imaged at the field lens, and not at the detector, the aberration becomes unimportant. The parameters available at the mirror are mirror diameter and radius of curvature. The larger the radius of curvature, the larger the solar image, and the more energy it contains. Maximizing this radius is not desirable, however, since as the radius of curvature increases, the amount of image motion produced by a given satellite attitude control error also increases. Thus, with increased diameter of the solar image forming mirror, the energy available within the system becomes very large, but the system becomes extremely sensitive to attitude control errors. In the present system, the radius of curvature chosen is about 5 cm, which gives an effective focal length for this mirror of 2.5 cm. The diameter of the mirror is about 1.25 cm, which permits at least a $\pm 5^{\circ}$ ($\pm$ 0.088 radian) attitude error before vignetting takes place at this mirror.

Spectrometer section. — It is necessary that at least part of the energy which returns from the sample in the solar channel be divided into its spectral components for a rough check on the spectral reflectivity of the sample. One straightforward way of accomplishing this task would be to replace the elemental detector with an array of detectors, each covered with a filter of appropriate bandpass. This scheme is probably the simplest and lightest possible, but it suffers from the vagaries of filter technology. Thin film filters would be the most predictable in manufacture, but they were not considered because they would probably be too sensitive to repeated temperature cycling, such as would be encountered in an orbiting satellite. Solid glass filters were also considered, but the bandpasses desired could not be found as catalog items. Reflective defraction gratings would provide another possible, it not feasible, solution. No single grating could be used over the wide wavelength range necessary here, since overlapping orders of spectra would be troublesome. Four separate gratings, having different spacings, would be necessary. This would be considerably more expensive and certainly more difficult to fabricate than the solution finally used.

The solution finally chosen is shown schematically in Figure 5. The image of objective lens (as in Figure 3) is formed at the entrance slit of the spectrometer and acts as a source for it. Lens C collimates

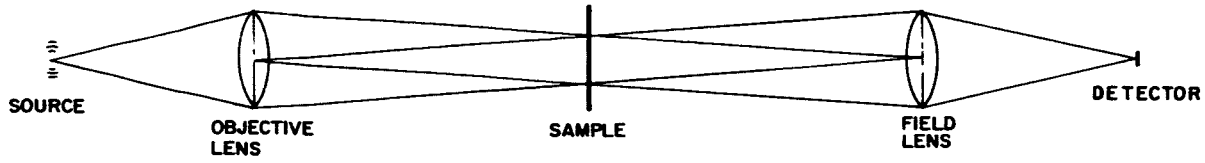

FIGURE 3 BASIC SYSTEM

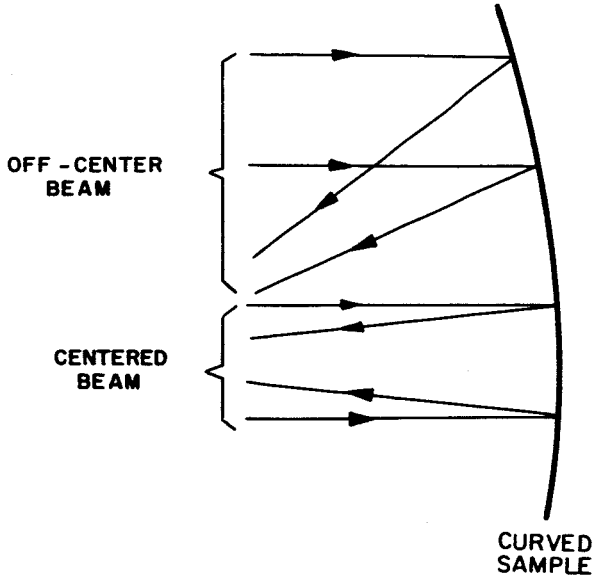

FIGURE 4

EFFECTS OF SAMPLE CURVATURE

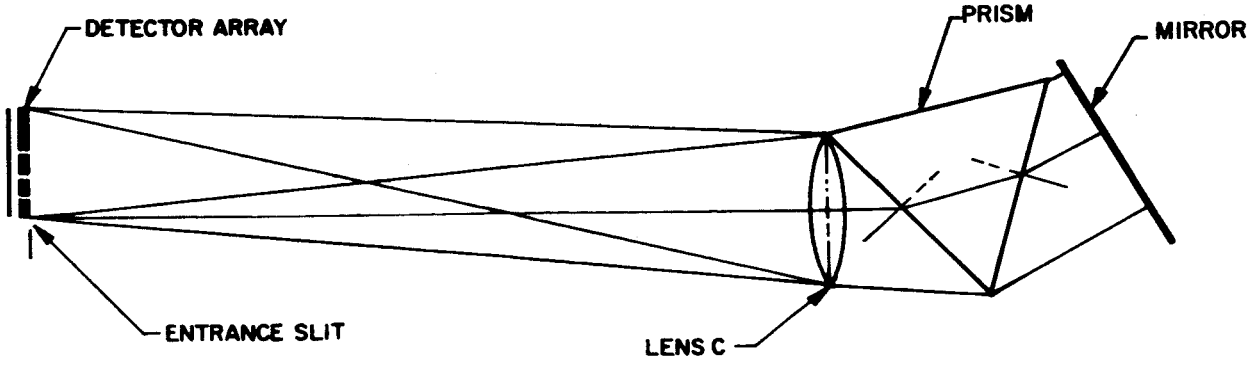

FIGURE 5 SPECTROMETER ASSEMBLY

the energy from the slit. The beam then passes through the prism, reflects from the mirror, and passes back through the prism again. Lens C then forms an image of the slit, spread out into a spectrum by the two passes through the prism. The prism is a 60° (1.05 radian) quartz prism which is aligned to the angle of minimum deviation at 2.0μ. The angle of incidence at the first surface is 45.9° (0.80 radian), as is the exit angle from the second surface, at this wavelength. The mirror returns this beam on itself, and the exit beam from the forth surface is parallel to the original entrance beam. Table I lists the refractive index of fused quartz as a function of wavelength, together with computed exit angles after two passes through the prism. Based on these angles, the 15 cm focal length spectrometer lens will produce a spectral spread of 2.3 cm at the detector plane, for the range 0.3 - 2.0μ. The requisite spectral resolution is produced by limiting the slit width to 1.25 mm. This gives sufficient signal at the detector outputs without seriously degrading the resolution of the spectral measurements. This slit width represents approximately 0.04μ resolution at 0.45μ, and about 0.3μ at 2.0μ. Four uncooled lead sulphide detectors are used in the spectral detector array, three of 4 x 4 mm size, and one of 5 x 10 mm size. Nominally, the spectral regions covered are 0.3 - 0.45μ, 0.45 - 0.65μ, 0.65 - 1.22μ, and 1.22 - 2.0μ.

TABLE I

REFRACTIVE INDEX OF FUSED QUARTZ
AND PRISM EXIT ANGLES (REF. 1)

λ	n	Exit Angle (degrees)	Exit Angle (radians)
0.30	1.488	55.0	0.940
0.35	1.478	53.0	0.925
0.42	1.468	51.1	0.892
0.61	1.458	49.3	0.860
1.20	1.448	47.6	0.831
2.02	1.438	45.9	0.801

Complete optical system. — A schematic of the complete optical system, lacking only the additional mirrors necessary to fold it for more compact packaging, is shown as Figure 6. Both the solar energy system and the tungsten source system are shown in the figure. The two systems are interlocked in such a way that the objective lens for one system is the field lens for the other system, and vice versa. In the solar energy system, Lens A acts as the objective lens, and Lens B acts as the field lens. These two roles are reversed in the tungsten system. For ease in drawing layout, the system is shown "unfolded" around the sample, so that in the drawing the light apparently passes through the sample. Actually, of course, the light beam bounces off the sample in every case.

Tracing through the system, the sun's energy enters from the upper left and is focused by the concave reflector to the image shown. The energy from this image passes through beamsplitter A, through lens A, off the sample, through lens B, then off beamsplitter B. Part of this energy falls upon the white light detector and part of it passes through the slit aperture for measurement in the spectrometer section. The tungsten source is shown at the far right of the diagram. Energy from this source passes through beamsplitter B, through lens B, off the sample, through lens A, and is reflected from beamsplitter A to the "white light detector for tungsten" which is shown in the diagram. Two choppers are shown in the figure, but the system is folded in such a way that these are actually two parts of the blades of a single tuning fork proper.

With the addition of sufficient mirrors to package the system realistically, it gets somewhat more complex. Figure 7 shows the folded system, for one arm position, together with rays indicating the path of the energy from the tungsten source. The additional components shown are the arm mirrors M_4 and M_5, pathfolding mirrors M_1 and M_6, and windows W_1 and W_2. Figure 8 is a similar diagram, but including the rays for the solar energy system instead. Mirrors M_4 and M_5 as well as window W_1, are located in the arm and hub and rotate with it as it scans. Window W_2 is the solar window in the top plate, through which the sun's energy enters the reflectometer. While lenses A and B are mounted up within the hub of the reflectometer, they are not fastened to the hub, but are mounted in a tower which rises from the baseplate which also supports many of the other components shown.

The return beams from the tungsten system and from the solar energy system cross as they go through the chopper which is indicated only schematically in the figures. This unusual folding of the beams permits use of a single chopper for both solar and tungsten systems.

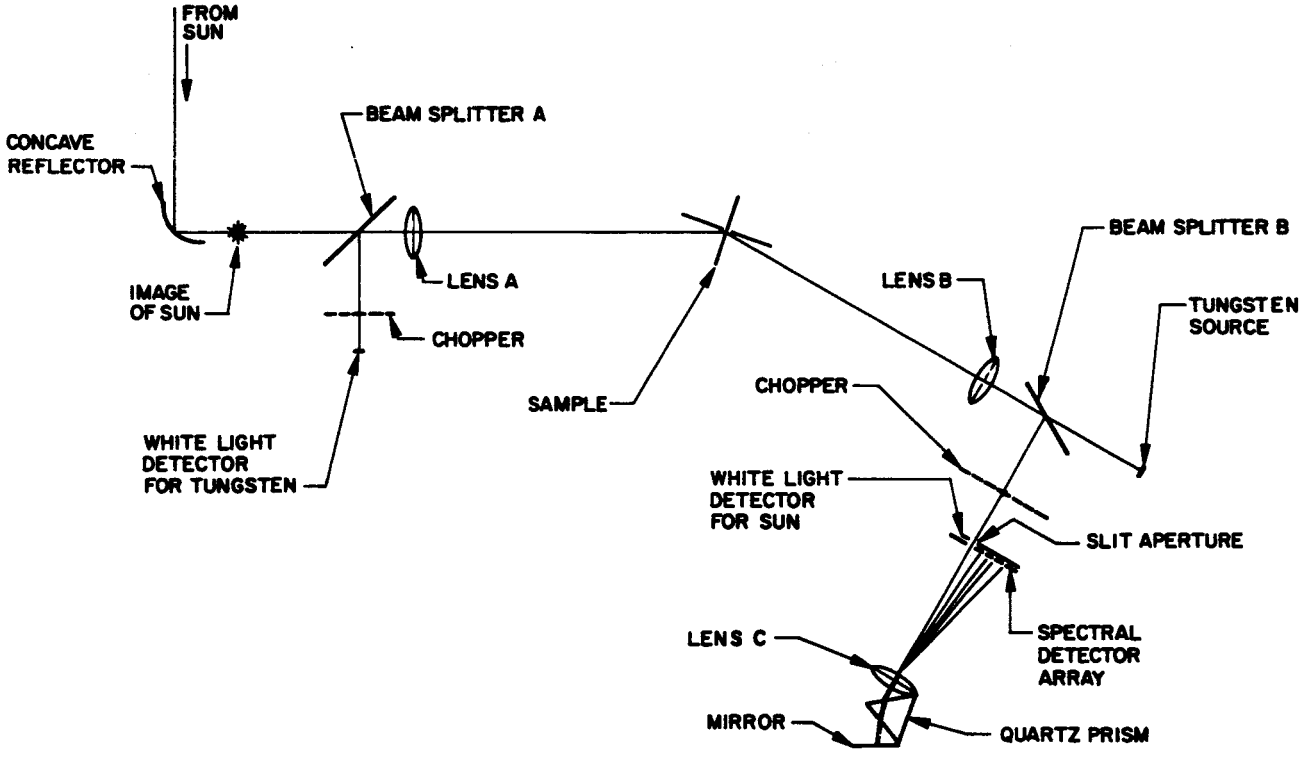

FIGURE 6 NEW OPTICAL SYSTEM

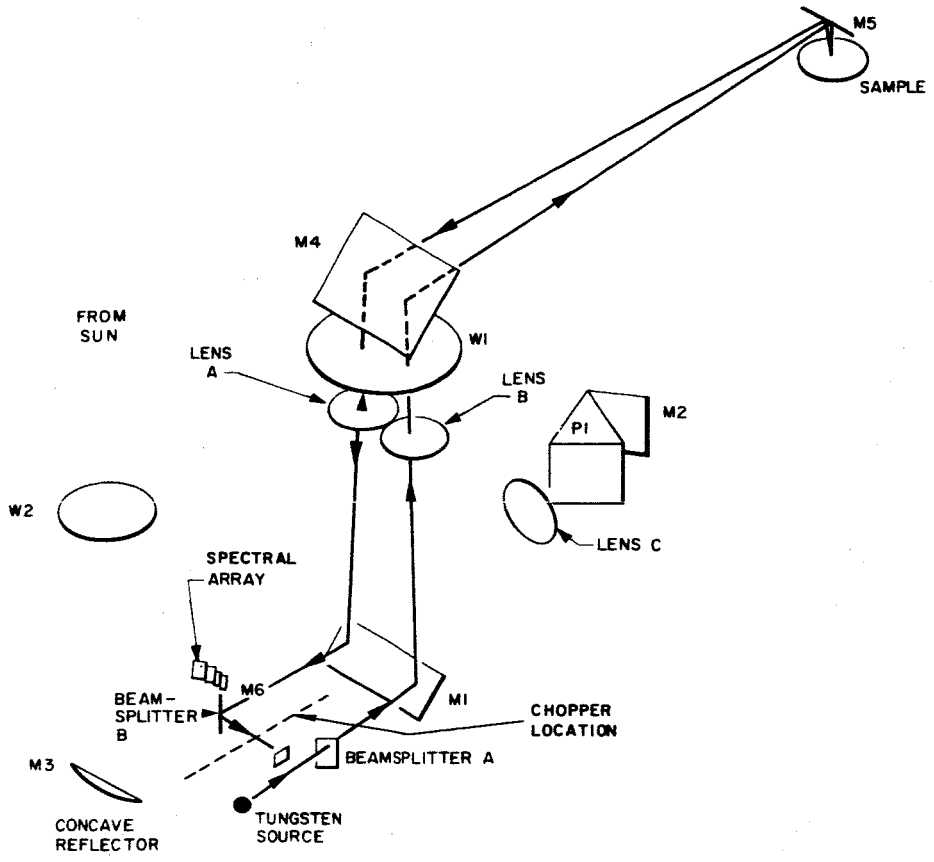

FIGURE 7 OPTICAL COMPONENT LOCATION (TUNGSTEN SOURCE)

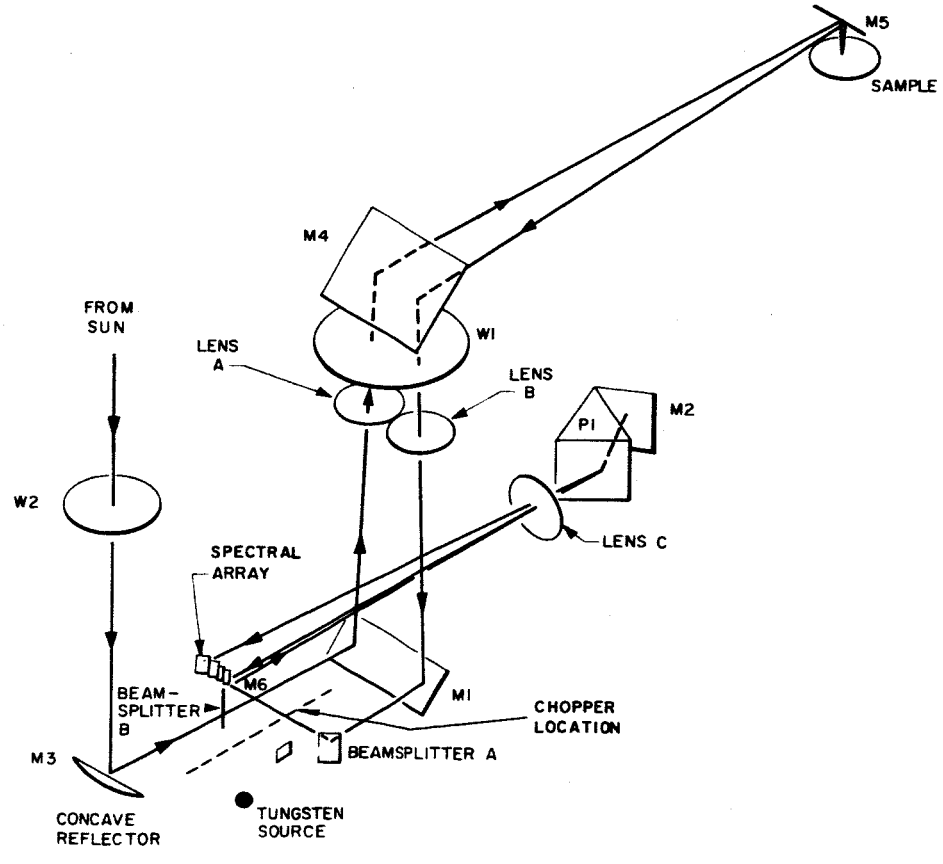

FIGURE 8 OPTICAL COMPONENT LOCATION (SUN SOURCE)

All of the transmitting optical elements in the systems shown are of fused quartz, to permit transmission in the near ultraviolet. Fused quartz is an extremely stable material which withstands the rigors of the space environment better than ordinary glasses, hence it is used as the substrate for mirrors M_4 and M_5 as well. Its use for windows W_1 and W_2 is also dictated by its resistance to the space environment, since in a flightworthy model these windows would be the seal between the interior of the reflectometer and the space vacuum. W_1 is tilted about 3^o relative to the hub axis to help prevent spurious reflections within the system. Window W_1 and W_2 are approximately 3.8 mm thick. Assuming atmospheric pressure within the instrument and a hard vacuum without, this will provide a factor of safety of at least 10 before breakage occurs because of the pressure differential.

Calibration. – In the measurement of the specular reflectance, one of the key prerequisites is a precise method of calibrating the instrument used. In the rotating arm reflectometer, the method used is to have two samples of known reflectance mounted with the other samples on the periphery of the disc. In this prototype, the standards are a fused quartz prism (which uses the phenomenon of total internal reflection to achieve a high, constant reflectance) and a dummy sample painted with a highly diffusing black coating. The normal rest position of the reflectometer arm of a flightworthy instrument would be over these two reference samples, protecting them. The use of reference samples in this way allows calibration for full scale deflection once during each cycle, thus greatly enhancing the certainty with which the quantitative reflectance measurements can be regarded. By calibrating for full scale reading once during each cycle, drifts in detectors, amplifiers, light sources, and telemetry are rendered relatively unimportant.

The actual reflectances of the roof prism and the black cavity are not precisely 100 percent and zero, respectively. However, the prism and the black cavity have reflectances which can be measured in the laboratory and which are not expected to change appreciably in the space environment, particularly considering that they will be protected during most of the flight. The stability of the prism is derived from two features:

1. It is made of quartz which is relatively immune to space environmental effects.

2. A reflection occurs by total internal reflection within the prism. It does not depend on the use of any surface coatings which might degrade.

While the 100% prism is extremely stable in reflectance, calculations indicate that it should be quite sensitive to modest misalignments. The index of refraction of fused quartz is so low that for a roof prism

such as the 45°-45°-90° (0.78-0.78-1.57 radian) prism used here to exhibit total internal reflection, the impinging radiation must be almost normal to the hypotenuse face of the prism. The value of "almost" depends on the wavelength of the radiation. Table II indicates the maximum angle of incidence at the hypotenuse that will yield internal reflection for the prism.

TABLE II

ANGLE OF INCIDENCE VS WAVELENGTHS
FOR -100% CALIBRATE PRISM "REFLECTION"

λ (μ)	Angle of Incidence (degrees)	Angle of Incidence (milliradians)
2.0	1.35	23.6
1.6	1.65	28.8
1.2	1.81	31.6
0.8	2.21	38.6
0.6	2.48	43.3
0.4	3.15	55.0
0.35	3.53	61.6

In the case of the tungsten source and proper alignment the beam geometry is as shown in Figure 9. The angle which each of the extreme rays makes with the optical axis in this case is

$$\text{TAN}^{-1}\,\frac{2.54 + 0.38}{2\ (64)} \cong 1.31^{\circ}\ (0.0229 \text{ radian})$$

Thus, total internal reflection is achieved in a perfectly aligned system for wavelengths up to about 2.06μ and no farther. In the presence of moderate misalignments, it is thus apparent that the reflectance of the prism might drop considerably below 100 percent, but to the extent that the misalignment remain constant, the effective reflectance of the prism would also remain constant. Given particular misalignments, and given also the distribution of irradiance in the image, it takes only a rather straightforward but tedious graphical integration to yield the polarization reflection coefficients of the prism for any particular wavelength. It should suffice to know here that accurate alignment is a necessity if the prism is to be regarded as a "100%" sample up beyond the visual range of the spectra. It should also be emphasized, however, that while the prism may not represent a 100% sample, it does represent a stable standard.

Electronic System

Basic considerations. — The electronic requirements for the prototype reflectometer are relatively straightforward. A control box is provided which provides the necessary switches and selectors to operate the prototype, a solid-state power supply which converts 115 Vac, 60 cycle power to 24 Vdc power used in the instrument, together with an output meter and necessary switching and indication circuitry. The power supply mentioned is a relatively heavy one, and represents what would be batteries and/or solar cells on an orbiting satellite. It is placed within the control box so as not to penalize the weight and volume of the prototype instrument by including parts that would logically be in the parent satellite of an airborne instrument. All other functions which would be performed in a flightworthy instrument are contained in the prototype.

A system block diagram is shown as Figure 10. The area to the left of the dotted line represents the control box and the area to the right the prototype proper. A "scan" command from the control box closes a relay in the reflectometer which applies 24-V power to the tuning fork drive circuit and to a threshold sensor circuit. While the tuning fork proper is attaining its full amplitude, a process which takes 15 - 30 seconds from a stationary start, no other power is applied to components within the prototype. The threshold circuit shown monitors a reference output from the tuning fork drive circuit and closes the power relay shown when this reference output has attained sufficient amplitude. The amplitude of this reference output is proportional to the amplitude of the tuning fork oscillations. When the power relay closes, the 24-V power is applied to the tungsten lamp, to the arm drive motor, and to the detector-amplifier circuitry. Thus, the lamp and motor circuits, which would represent the largest part of the instrument power requirements of an orbiting instrument, are not activated during the warmup period of the chopper. Each of the six detector-amplifier-rectifier channels of the prototype is identical, with the exception of the tungsten channel. This channel omits a passive bandpass filter which is used in each of the other channels to increase the signal-to-noise ratio.

Detectors. — The detectors used in this prototype are uncooled photoconductive lead sulphide cells similar to the ones used in the previous optical model. Lead sulphide cells provide extremely lightweight, low-bias power requirements, and good detectivity and spectral response. While these detectors are ordinarily used mostly in infrared applications, the detector manufacturer had confirmed that their response extended well down into the ultraviolet region (see Figure 11) and hence they were suitable for use in this application.

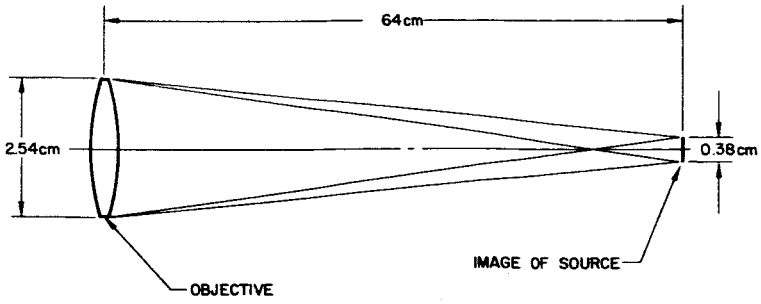

FIGURE 9

BEAM CONVERGENCE

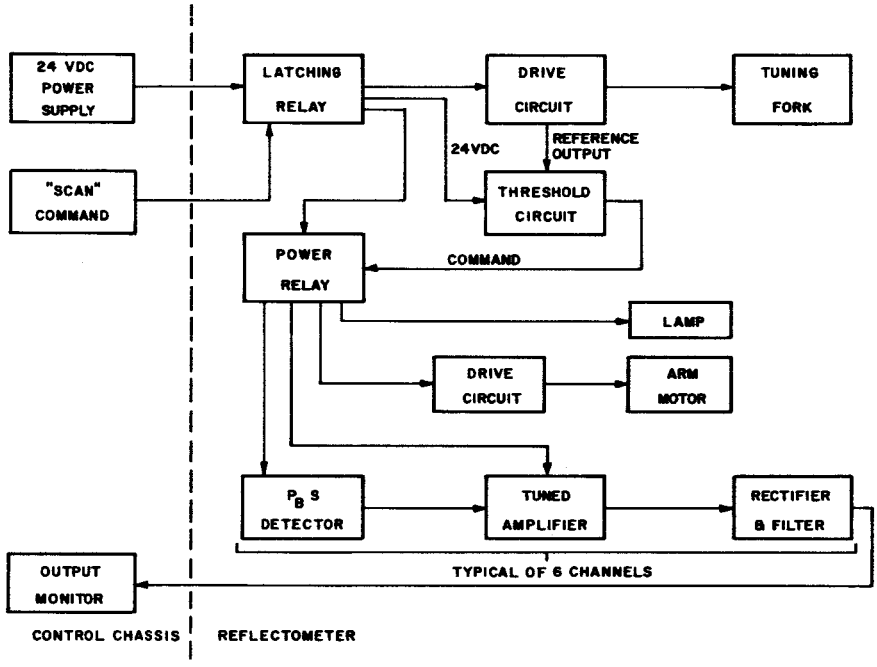

FIGURE 10

SYSTEM BLOCK DIAGRAM

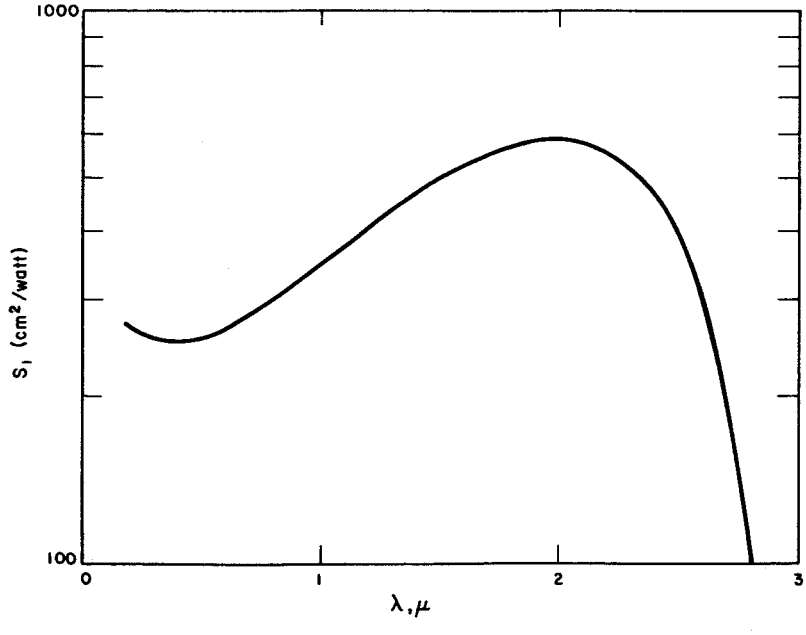

FIGURE 11

SPECIFIC RESPONSIVITY OF TYPICAL LEAD SULFIDE DETECTOR

Four-by-four millimeter detectors have been used in every case except in the "blue" spectrometer channel. The spectrum is so widely spread in that case that a five-by-ten millimeter detector is necessary there. In every case the active detector has a paired "blind" detector which is shielded from the light, and which is electrically in series with the active detector. Lead sulphide detectors are markedly temperature sensitive, but this bias configuration produces a matched load over relatively wide temperature variations, and largely eliminates spurious signals caused by temperature changes. Active and blind detectors in each channel are matched in resistance to within 10% at room temperature.

Amplifier channels. - The lead sulphide detectors used in the prototype have a nominal resistance of approximately 0.5 megohms/square, a reasonably conventional value for uncooled lead sulphide. This rather high impedance presents a problem when coupling to a conventional transistor amplifier, since the amplifier input impedance is apt to be lower than this by a factor of from 10 to 100. The field effect transistor (FET), a relatively new member of the transistor family, offers an extremely high input impedance compared with other transistors. For that reason an FET pre-amplifier has been used in the prototype. A schematic is shown in Figure 12. The input resistors fix the bias at the gate of the FET, and the emitter follower output stage permits the FET to work into a relatively large load resistor, for increased gain. The voltage gain of the two-stage circuit as shown is about 10. Five of these pre-amplifiers are packaged with the five solar channel detectors in a single small block. This configuration permits use of the high impedance at the interface of the detector and the pre-amplifier without the pickup noise problems that would be encountered if they were mounted remotely from each other. While the detector for the tungsten channel is mounted at the side of the tuning fork chopper, its pre-amplifier is mounted several centimeters away. This arrangement is satisfactory in this case because of the larger signal levels involved.

In the solar channels, the FET pre-amplifier feeds a modular band-pass filter which is tuned to 105 cps, the fundamental frequency of the fork vibrations. Filter input and output impedances are 10 kohm and 40 kohm, respectively. The 40 kohm output effectively matches the input impedance of the following power amplifier. In the tungsten channel the filter is not used, but the pre-amplifier feeds the power amplifier directly.

The power amplifiers are modular, four-transistor ac-coupled amplifiers. They are supplied with an open feedback loop which is closed resistively, in this case, to provide stable amplification. The blue solar channel carries fixed feedback producing an amplifier with a gain of 100 dB, the maximum recommended by the amplifier manufacturer. Each of the other amplifier channels has a multi-turn pot to allow reasonably easy control over the amplifier gain.

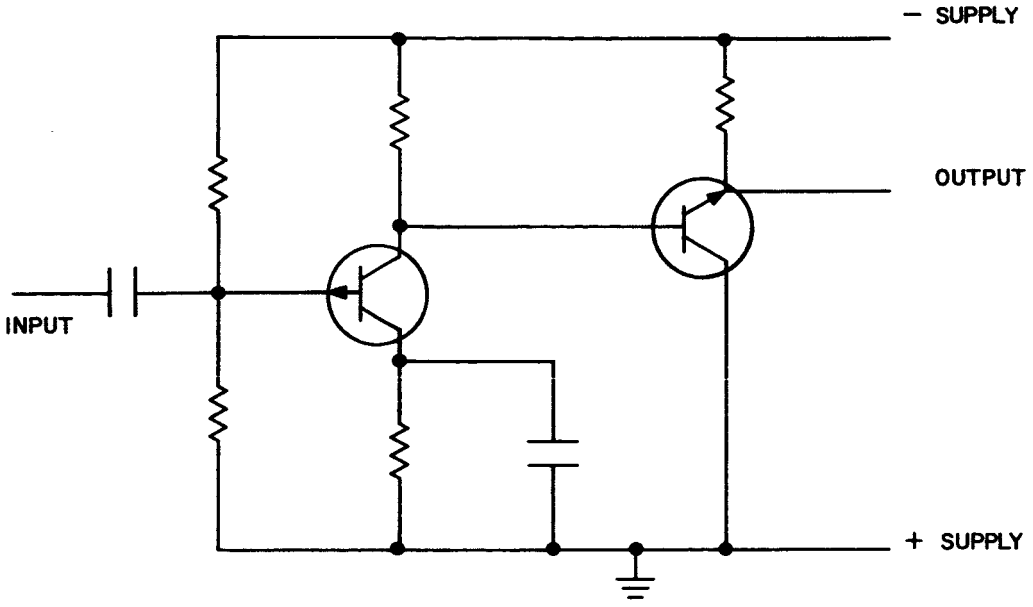

FIGURE 12 FET PRE-AMPLIFIER

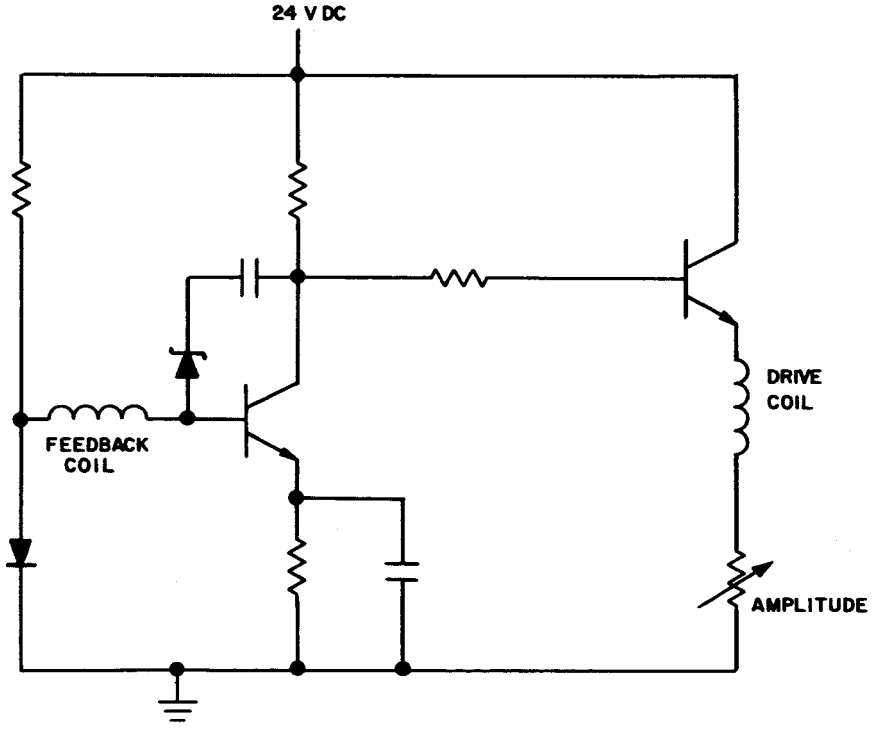

FIGURE 13 TUNING FORK CHOPPER CIRCUIT

The six power amplifiers are run directly off the power supply bus. The FET pre-amplifiers are separated from the amplifier bus by a single section of rc filtering, to eliminate feedback-generated oscillations.

Rectifier-Filter. - The output of each amplifier stage is capacitor-coupled to a step-up transformer which feeds, in turn, a full wave rectifier. Filtering at the rectifier output is provided by a single capacitor, which was chosen to limit the peak-to-peak output ripple to about 10% of the dc level present. This produces a usable dc signal without prejudicing the transient response at the output of the amplifiers.

Tuning fork & control circuitry. - The tuning fork chopper is a conventional tuning fork with two additional electrical coils, one to provide a driving force and the other to provide a sensing feedback. The manufacturer's tuning fork chopper drive circuit is shown as Figure 13. It is a two-transistor amplifier, with the second transistor being used to couple to the relatively low impedance of the drive coil. The reference output, mentioned above, is taken from the emitter terminal of the drive coil.

The threshold circuit used to close and latch the power switching relay comprises a voltage divider and a silicon-controlled rectifier. When the tuning fork drive coil voltage gets sufficiently large, the silicon-controlled rectifier fires and thereafter stays in a conductive state until the supply voltage is removed from it.

Mechanical Design and Packaging

General configuration. - The basic concept of the reflectometer's structure is shown in Figure 14. The basic package comprises three sections: the top plate, the base plate, and the arm and hub assembly. All of these parts are of aluminum. The top plate is a circular disc, 50.8 cm in diameter and 9.5 mm thick for most of its area. Near the periphery of the disc is an array of circular openings about 3.9 cm in diameter, into which the samples are mounted. For ease in alignment, each sample is mounted on a small triangular backing plate, which is fastened to the back face of the disc. These mounting plates are affixed to the disc by three screws, but are spaced from the back of the disc by O-rings placed between the mounting pad and the disc. The samples are thus, in effect, spring mounted by the compression of the O-rings. Tightening and loosening the mounting screws which hold the pad to the disc produces slight but sufficient adjustment of the plane of the sample.

Most of the optical components, as well as the electronics, are mounted to the base plate, which is held to the top plate by cylindrical aluminum standoffs. All of the optical components, except those in the

arm and the solar entrance window in the top-plate, are affixed to the base-plate. This allows the base-plate components to be aligned substantially independently of the top-plate and hub and arm assembly. This is a much more convenient arrangement than if the base-plate and top-plate had to be made early in the fabrication process and all of the optical alignment done thereafter.

The arm and hub assembly is the third basic structural component. The basic concept used here is portrayed in Figure 15. Two pre-loaded ball bearings of substantial bore permit the inner part of the hub to rotate relative to the outer part while maintaining the accurate alignment necessary for optical purposes. An hermetic seal is mounted in the seal area shown, between the inner and outer portions of the rotating hub, to prevent loss of internal reflectometer air pressure past this point. The slightly slanted plate shown in the center of the hub below the mirror represents quartz window W_1 (which is shown also in Figures 7 and 8), which seals off the possible air paths up through the center of the hub. A large spur gear is mounted to the bottom of the rotating section of the hub and driven by a dc gearhead motor mounted directly to the side of the hub housing. Assuming that these two gears are essentially frictionless, the available starting torque referred to the axis of rotation of the arm is 84 inch-pounds (9.5 meter-newtons). The seal installed in the prototype reflectometer hub (but not used, since the prototype is not otherwise pressure tight), has shown starting and running torques on the order of 20 inch-pounds (2.3 meter-newtons). Thus, the motor drive used provides a substantial factor of safety in case of a marked increase in seal or bearing friction.

The choice of motor for driving the hub of a flightworthy reflectometer would depend, in a large measure, on the leakage rates attainable with the seal chosen. One manufacturer specifies that his brushes will operate satisfactorily at altitudes as high as 30.5 km, which corresponds to an ambient pressure of about 8 torr (1.1×10^3 newton/meter^2). In the case that an ac motor were used, with its attendant dc to ac converter, the internal pressure necessary at the end of the mission would be considerably less, and the seal requirements correspondingly less stringent. An ac gearhead motor and converter combination would be more expensive and somewhat heavier (minimum penalties would be on the order of $1000 and 0.34 kg, respectively) but in the case of catastrophic loss of all pressurization inside the reflectometer, a properly lubricated ac motor would continue to operate while a dc motor would fail quickly. Since the change to an ac motor-converter would be a relatively straightforward one, and in view of the market cost difference, a dc gearhead motor was chosen for the prototype. Mounted as it is, directly to the side of the stationary portion of the hub, the mechanical drive path is very short and stable. The motor has been wrapped with magnetic shielding foil, and the line filter is used between the motor and the power supply to help reduce the inevitable brush noise.

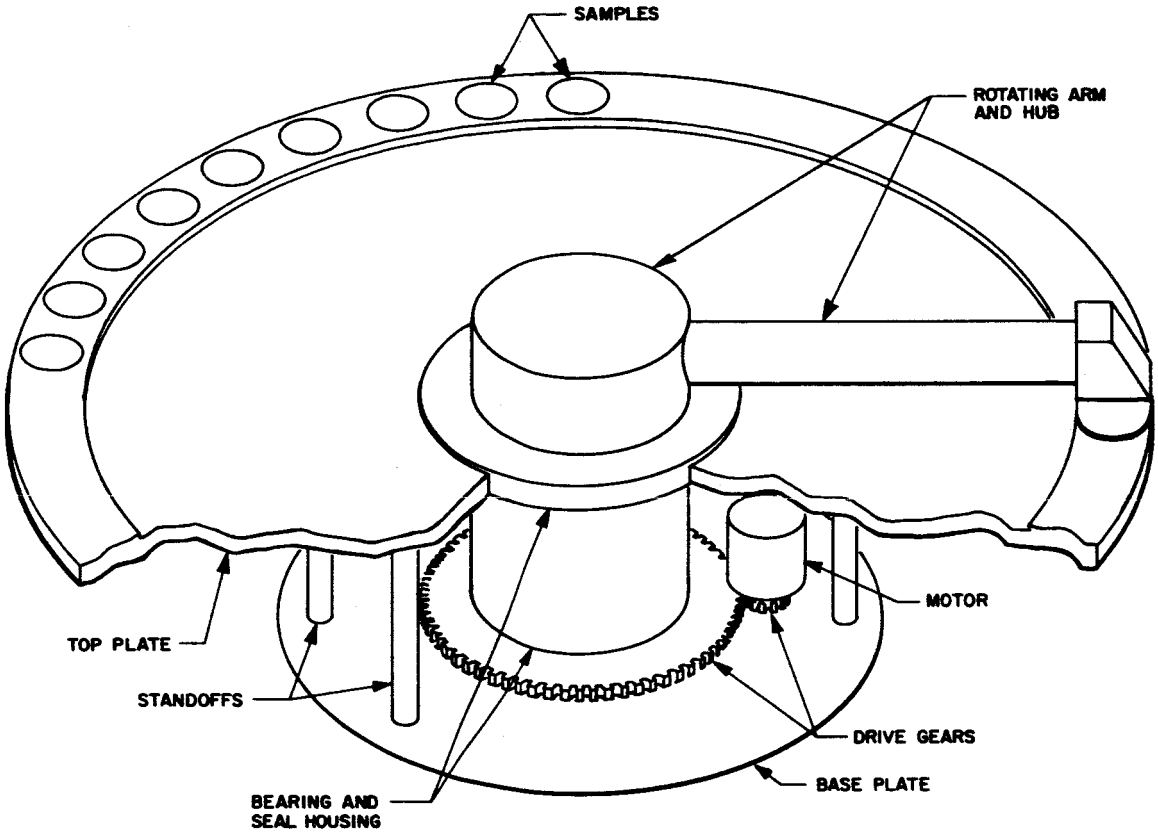

FIGURE 14 STRUCTURAL CONCEPT

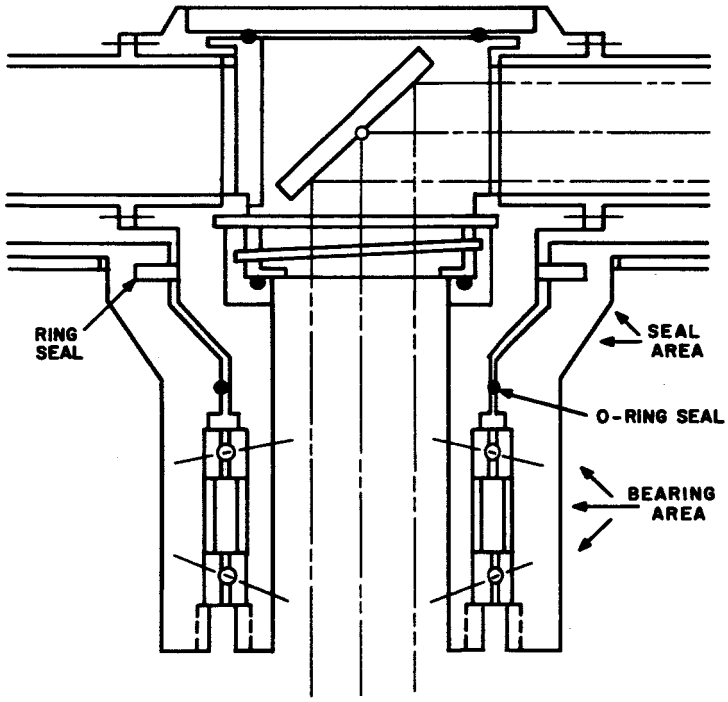

FIGURE 15
ARM-HUB CONCEPT

All of the electronic components, with the exception of the tuning fork, the tungsten source, and the solar detectors, and pre-amplifiers, are mounted on an irregularly shaped bracket which in turn is mounted to the base plate. The configuration of the electronics bracket was chosen to keep the center of gravity of the base plate close to its geometric center.

The base assembly is covered by a coffee-can-shaped dust cover, attached to the upper disc, and surrounding the base assembly but not touching it. As well as acting as a dust cover, this simulates what we presently envision to be the most feasible method of hermetically sealing a flightworthy model.

The optical mountings have been designed with as few degrees of freedom as possible, consistent with being able to align the reflectometer components. The three lenses, both windows, and the spectrometer prism are all either cemented or clamped into their cells, which are not adjustable. In all other cases, the optical elements are mounted in cells which are slightly adjustable with respect to the basic structure. The two beamsplitters and the lateral mirror M_2 are mounted in cells which can be adjusted around three orthogonal axes. The vertical axis is gimballed to permit a relatively wide range of adjustment, while alignment in the other two axes is provided by push-pull screws.

Assembly and Alignment

Base plate assembly. - Optical alignment of the entire system was accomplished using a laser beam as an alignment tool, as was done with the first prototype reflectometer. The high brightness and small diameter of the laser beam render it invaluable as an alignment tool with reasonably complex optical systems like that of the prototype.

Optically, the only function of the arm is to permit substitution of one sample for another by moving the reflectometer beams. If the arm-disc assembly is properly aligned, the base assembly "sees" the sample as though the sample were suspended horizontally face down in midair above the center of the base assembly. To facilitate optical alignment, an adjustable ring stand was used to hold a mirrored precision optical flat 45.5 cm above the bottom of the base plate. This flat was thus in the same optical position as a sample would be. The laser beam was then aligned 1.83 cm above the top of the base plate and parallel to it. This was the nominal height for all of the horizontal beams in the reflectometer. Using the laser, the optical elements were then installed in the following order: M_1, lenses A and B, the chopper, beamsplitter A, M_6, and the spectrometer elements.

The tungsten lamp was then installed, as well as beamsplitter B, and the latter was adjusted until the image lens B was properly centered on the tungsten detector. The spectrometer mirror was adjusted until the spectral image of the entrance slit was centered vertically on the detectors, and the narrow red line from the 0.63μ laser was seen just at the "red" end of the 0.45 - 0.65μ detector.

Alignment of the hub-arm sample assembly was done before mating it to the base assembly. Before the disc was fastened to the hub, window W_1 and mirrors M_4 and M_5 were installed, and a mirrored flat placed over the arm aperture near M_5 to simulate a sample. Arm alignment was then done by looking up into the hub and moving M_4 until the apertures seen were concentric. The extra alignment mirror was then removed from the end of the arm, and the disc with its samples was attached to the hub. The assembly was then inverted, and a mirrored optical flat placed over the hub aperture. The laser beam was auto-collimated from the center of this mirror, then the mirror was removed and the sample adjusted until auto-collimation was again achieved. In the case of the reference prism, it was also necessary to align the prism radially until the prism axis of the prism was parallel, as seen through the arm, to what would later be the common center line of lenses A and B. This was necessary because a roof prism acts as a common mirror (incidence equals reflection) in one plane and is retrodirective (incidence equals minus reflection) in the other plane. If the prism were to be incorrectly oriented radially, so that the retrodirective plane contained the common center line of lenses A and B, the output beam from each lens would return upon itself, rather than being reflected to the other lens.

System Transmission

A modest transmission analysis of the type that had been done for the previous optical model was undertaken for the new prototype. Since the detailed procedure was well covered in the final report for the previous project, only a summary description will be given here. The general method involves setting up a pair of polarization axes, orthogonal both to the optical axis of the system (considering the system is completely unfolded) and to each other. Transmission of the system is then computed for polarized components parallel to each of these two axes, and the transmission of the system as a whole computed by combining these two components. In the case of the tungsten system, the transmission is exactly the same as that of the "ILS" system of the previous optical model, with the exception that the beamsplitter used here gives slightly higher efficiency (at least in the visual) than that used on the previous device. In each optical system, the beamsplitter is seen once in reflection and once in transmission. Thus, a beamsplitter efficiency criterion is the product of the reflection and transmission coefficients in each

polarization axis. In the present case, that product is 0.126 in one axis and 0.119 in the orthogonal axis. In the previous system, the transmission and reflection were measured, though not in polarized light, and in visual light the one-reflection/one-transmission coefficient was approximately 0.10. Thus, the transmission of the present tungsten system in visible light should be, overall, about 20% higher than that of the previous system, or about 5%.

A similar calculation was carried out for the solar energy system. Beamsplitter data had not been obtained spectrally, but only as a lumped measurement using a visual photometer, hence the calculations were carried to completion only at one wavelength, namely 0.50μ, where the photometric data should be satisfactory. Calculations indicate that at this wavelength the transmission of the solar energy system is about 4.6%, and that the modulation due to arm position is of the order of 2% of the average reading. If this calculation were carried out as a function of wavelength, the results expected would be approximately the same as those obtained on the previous project, with the transmission showing a drop of 30 or 40% in the 0.75μ region compared with the higher transmission in the ir region. While this calculation is of interest in predicting the approximate performance of the system, individual differences in the particular coatings applied would make detailed prediction difficult.

Testing

Test results for the prototype reflectometer were, in general, gratifying. Output signals were strong, stable, and with one exception, extremely noise-free. The control circuitry and arm-drive system were completely dependable, the mechanical structure of the reflectometer, including the optical mounts, was sufficiently sturdy and light to permit rather carefree handling, and the detector and signal processing electronics showed no embarrassing idiosyncrasies.

Since it is difficult to fabricate conveniently a laboratory source that will completely simulate the sun for test purposes, it was decided on this prototype, as had been on the previous optical model, to construct a heliostat, to permit use of the sun itself, rather than a simulated one. The heliostat built for the present program is a two-axis tracking device which uses two dc motors and dc closed-loop circuitry to position the heliostat mirror. The reflected beam of sunlight passes through an aperture in a plate mounted remotely from the mirror-drive assembly. Surrounding the aperture in the plate is an array of photo detectors which provide input signals to the servo circuitry to keep the beam centered on the aperture. The device was mounted on the roof of the building in which tests were performed, and the beam of sunlight sent down into the building through a hole in the roof. The

servo mirror was small enough so that the sun's image was sometimes vignetted, as seen from the instrument under test, but while this sometimes produced an apparent slow dc drift in the output signals, the convenience of having a "stationary" sun more than out-weighed this slight deficiency. Figure 16 shows a typical trace in the solar white-light channel.

One basic test run was to record the output of each channel of the reflectometer while the arm scanned the array of samples. Two repetitions of this test in the tungsten channel six hours apart revealed that the two traces were completely identical, to the accuracy with which a 4 to 5 cm deflection can be photographed on the face of an oscilloscope.

The tungsten channel test showed that the reflectance of the quartz reference prism in the tungsten channel was only about 75% of that of an adjacent silver-plated sample. This apparent violation of nature's laws probably had two basic causes. The first is that while this type of prism exhibits total internal reflectance for normal incidence well into the infrared, the impinging beam is sufficiently convergent so that the beam is theoretically totally reflected only for wavelengths shorter than 2.06μ. Since the tungsten source has considerable energy above this wavelength, and since the lead sulphide detectors are nominally sensitive up to around 3.0μ, a sizeable portion of the tungsten energy excapes through the prism, rather than being reflected from it. The reflective samples, however, remain reflective over the entire effective spectrum. Examination of the transmission curves of the fused quartz, from which the reference prism was fabricated (see Figure 17), reveals also that this particular quartz exhibits a rather sharp drop in transmittance, starting just under 2.0μ. This dip is caused by absorption bands in water entrapped in the quartz.

In order to test the effect on reflectance measurements of sample curvature, a special double-sided sample had been made of glass, then aluminized. This sample has a focal length of +254 cm on one side, and -254 cm on the reverse. Comparative scans were run in which the only difference was that the convex side of the sample was up in one case, and the concave in the other. The convex and concave readings varied respectively ±21% from their mean in the tungsten channel, and ±14% from their mean in the total solar energy channel. This does not represent the complete freedom from sample geometry effects that would be desirable in a flightworthy reflectometer, but it does offer a considerable improvement over the spectral confusion resulting from sample power which was encountered on the first optical model. While we have not analyzed the situation completely, it appears that the change in indicated reflectance for a curved sample is approximately the same as the change in irradiance that would be produced at the detector by adding or subtracting an equivalent amount of optical power. The effect can thus be thought of as being produced by a change in magnification between the objective lens and the image of the objective lens formed at the detector by the field lens.

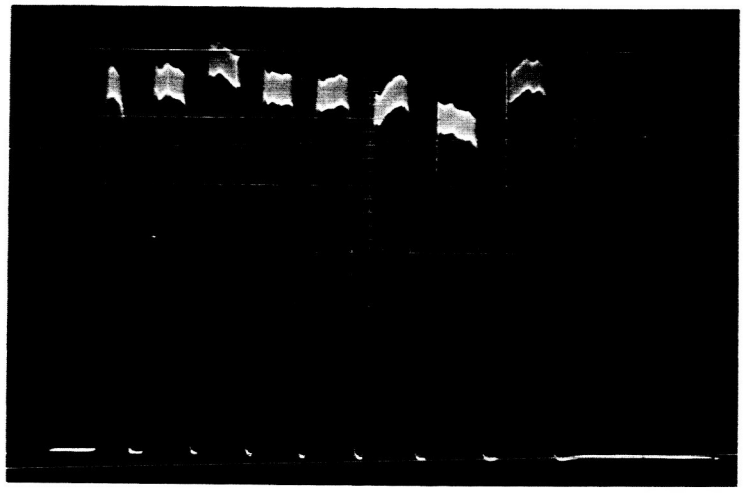

FIGURE 16 TYPICAL OSCILLOSCOPE TRACE IN SOLAR WHITE-LIGHT CHANNEL

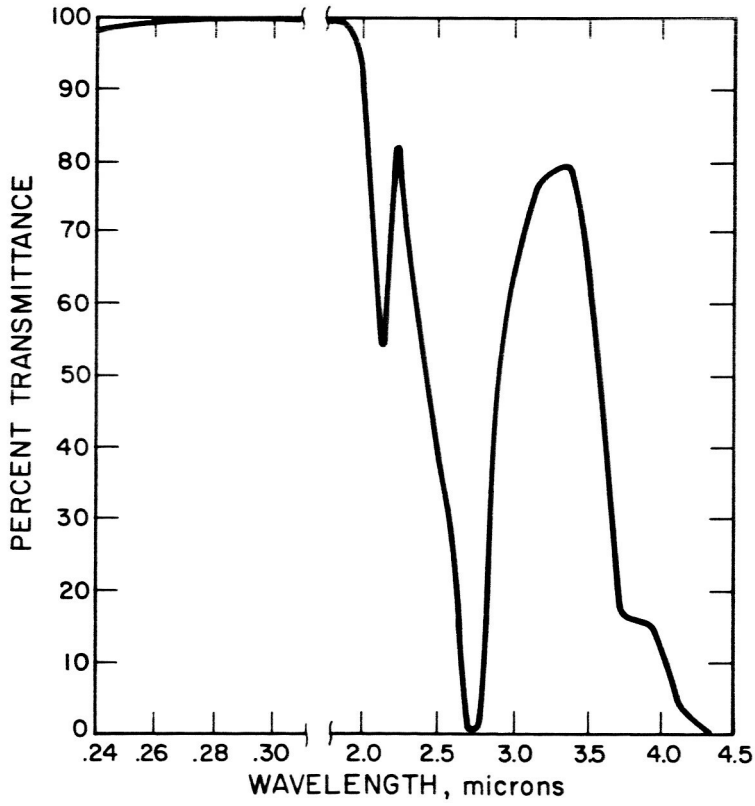

FIGURE 17 TRANSMITTANCE CURVE - FUSED QUARTZ FOR 1 CM THICKNESS (excluding surface reflection losses)

This change, produced by sample geometry, would be a real constraint on experiment precision and accuracy unless compensation were made for it. It is evident that some surface-substrate combinations would be particularly sensitive to geometric changes with temperature. If these were to be tested, it would be mandatory to obtain temperature-curvature curves on the particular samples used, and to monitor the temperature of the samples during the flight experiment. It would also appear desirable to mount the samples by stress-free mounts, which would prevent the change of sample geometry from sources other than temperature.

Spectral calibration of the spectrometer section of the prototype could not be performed directly, since this would have required construction of an ultra-violet to infrared monochromator of sizeable power output, an effort which was beyond the scope of the test program. Since the intent of the spectrometer section is not a detailed, high-resolution measurement but rather a broad-gage one, it was deemed sufficient simply to note the output of the spectral channels with spectral filters inserted into the light path. Two filters were used: a long-pass filter cutting on at about 0.75μ, and a short-pass filter giving transmission from about 0.65μ down. The data are summarized in Table III.

TABLE III

SPECTRAL OUTPUTS WITH INPUT FILTERING

Channel	Output Without Filter, Volts	Output With Short-Pass Filter, Volts	Output With Long-Pass Filter, Volts
0.3-0.45μ	2.0	0.2	1.3
0.45-0.65μ	2.0	1.6	0.3
0.65-1.2 μ	2.0	0.0	1.4
1.2 -2.0 μ	2.0	0.0	1.7

The disturbing feature here is the apparent connection between the 0.3-0.45μ channel and the ir channels. We feel that this cross talk is optical, and represents stray light in the system. This situation is complicated by the high gain necessary in this channel, since even minute amounts, proportionately, of infrared radiation represent large signals compared to the tiny amount of ultra-violet radiation being sought here. A straightforward solution to this problem would be to add a short-pass optical filter in front of the ultra-violet detector. This problem would not arise in an orbiting instrument, since the ultraviolet level above the atmosphere would be much higher.

Attitude sensitivity of three of the solar channels was tested by using a slide projector, minus its heat shield glass, as a solar simulator. This projector was set up so that it was at the focus of a reflective

collimator of 2.7-meter focal length. The prototype reflectometer was then set up in the beam, and the outputs of the solar white light and the two solar infra-red channels were monitored while the prototype was moved in the beam. The prototype was turned around each of two axes which are shown schematically in Figure 18. Positive rotation is defined by the right-hand rule.

The results of these manipulations are shown in Tables IV and V for the X and Y axes, respectively. The zero-degree position in each axis is not necessarily exact, but represents only an approximate reference position. While the attitude control error which can be tolerated varies from channel to channel, satisfactory signal levels can be obtained over an 8° (0.14 radian) range in the X axis, and about a 6° (0.10 radian) range ($+2^{\circ}$ to -4°) in the Y axis. The skewed Y-axis response curve in the 0.65 - 1.2μ channel was not investigated. It may be connected with chromatic aberration in the optical system.

The transmission of the optical system changes slightly with arm position. This phenomenon has been treated analytically by considering the reflection polarization coefficients of the various system components as the arm rotates. It was originally intended to perform an experimental check on the theoretical result, but no straightforward method was found to produce experimental results with the entire system which could be thus correlated with theory. One test which was performed was to place a sheet of linear polarizing material over the sun port and then run a scan in the 0.45 - 0.65μ channel. This scan showed marked modulation, with the smallest signal being only about 30% of the largest one. The polarizer was parallel to the X axis of Figure 18 and the minimum apparent reflectance was produced when the arm axis was also parallel to the X axis.

Apparent output modulation was noted on the tungsten channel outputs with arm rotation, but since this modulation is about 5% peak-to-peak of the average value, as against the 2-1/2% that the transmission theory would predict, we feel that the apparent modulation is actually caused by random differences in the surface reflectivity of the various samples. Further, the apparent "modulation" has an approximate period of about 90° ($\pi/2$ radians) of arm rotation, whereas the transmission-induced modulation would have a period of 180° (π radians).

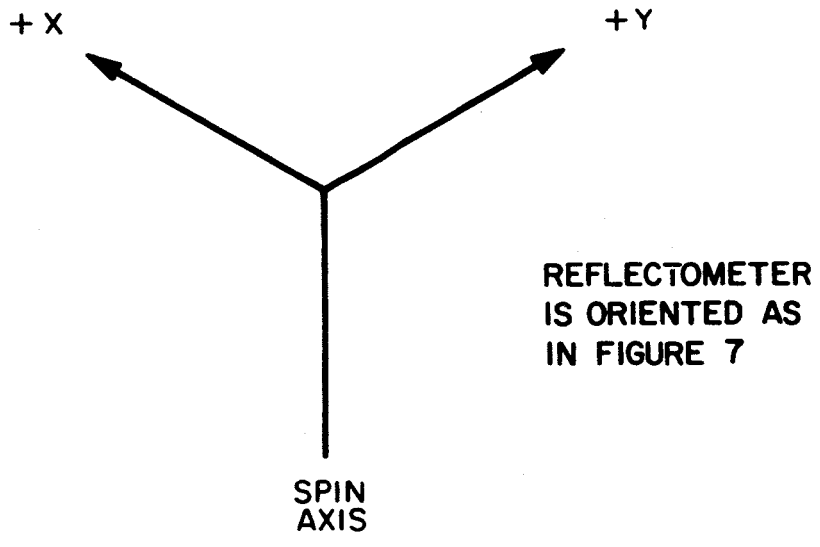

FIGURE 18 REFLECTOMETER REFERENCE AXES

TABLE IV

OUTPUTS WITH ATTITUDE CHANGE IN X AXIS

(Sample: Cr + SiO + Al + SiO_x)

X (degrees)	X (milliradians)	Channel 2 (volts)	Channel 3 (volts)	Channel 4 (volts)
+10	+175		0.010	
+ 8	+140	0.000	0.22	
+ 6	+105	0.015	0.38	0.000
+ 4	+ 70	0.048	0.51	0.010
+ 2	+ 35	0.109	0.70	0.041
0	0	0.160	0.76	0.065
- 2	- 35	0.137	0.71	0.067
- 4	- 70	0.096	0.59	0.048
- 6	-105	0.020	0.47	0.028
- 8	-140	0.000	0.29	0.009
-10	-175		0.00	0.000

TABLE V

OUTPUTS WITH ATTITUDE CHANGE IN Y AXIS

(Sample: Cr + SiO + Al + SiO_x)

Y (degrees)	Y (milliradian)	Channel 2 (volts)	Channel 3 (volts)	Channel 4 (volts)
+ 4	+ 70		0.00	0.00
+ 3	+ 52.5	0.000	0.51	0.14
+ 2	+ 35	0.028	0.83	0.13
+ 1	+ 17.5	0.14	0.75	0.098
0	0	0.17	0.79	0.079
- 1	- 17.5	0.18	0.84	0.045
- 2	- 35	0.19	0.86	0.019
- 3	- 52.5	0.18	0.43	0.010
- 4	- 70	0.19	0.94	0.003
- 5	- 87.5	0.19	0.90	0.000
- 6	-105	0.18	0.88	
- 7	-122.5	0.17	0.68	
- 8	-140	0.00	0.00	

ROTATING HUB

Basic Considerations

In order to protect the drive motor and bearings necessary for the rotating arm from the hard vacuum of space, it is necessary to incorporate a seal in the hub assembly. A flight worthy instrument would be sealed shortly before lift-off, and the instrument would carry one atmosphere residual pressure within it as it entered orbit. By maintaining a leak rate low enough so that the internal pressure remains reasonably high during the life of the mission, the drive motor and bearings would operate without the vacuum-induced problems of lubricant evaporation. Such a seal would have a leak rate low enough to assure a substantial pressure within the instrument at the end of the mission, and still produce negligible friction to the drive system. The problem is to minimize the leak rate and friction level with materials that will withstand the hot-cold-vacuum-radiation environment of space without failure. Further, any outgassing products from materials used in seals should not be such as to coat the reflective samples. Since seal failure would leave the drive system exposed to a vacuum, a search was made for lubricants and lubrication methods that would permit continued bearing operation even if the space seal should fail. These lubricants would have the same no-outgassing requirements as the seal, since outgassed products within the reflectometer interior would coat the elements of the optical system, with catastrophic results. Table VI compares some of the salient properties of different types of lubricants. Several different oils and greases have been giving good results in vacuum environments in double shielded bearings using phenolic retainers.

In order to satisfy these requirements, a test fixture was fabricated for testing of rotating seals in a vacuum chamber. Further, weight loss tests were run in a vacuum chamber on several promising lubricants and seal material.

Seal Tests

A special test fixture was built for performing leak and friction level tests on the rotating seal. It comprises a heavy, hermetically sealed cylindrical container, about 50 cm in diameter, with a dummy hub assembly installed in its top. A 115 V ac, 60-cycle gearhead motor is mounted internally, and drives the rotating member of the hub through step-down gearing. With no load, the rotational speed is about 4 rpm.

TABLE VI

COMPARISON OF LUBRICANTS FOR SPACE ENVIRONMENT (REF. 2)

Lubricant	Advantage	Disadvantage
Oils or Greases	Information available on properties of lubricant, best choice for a given metal or metal combination; large choice of compounds; automatic replenishment at contacting surface.	Most of these materials have appreciable vapor pressure, and appreciable decomposition rates as compared to solid lubricants (dry film and self-lubricating materials).
Solid Films and Thin Metal Films	Low vapor pressure; no viscosity changes due to evaporation or changes in temperature; wide temperature ranges	No effective replenishment capability; hence they have a limited lifetime as compared to oils and greases.
Self-Lubricating Materials (Plastics, Leaded Bronzes, etc.)	Not sensitive to vacuum environment	Low load-carrying capability as compared to oil or grease lubricated metal bearings

As far as the seal and bearings are concerned, the dummy hub is exactly the same as the hub of the prototype. Figure 15 is thus illustrative also of the seal and bearing arrangement used on the dummy hub. The ball bearings shown offer good support to the moving member and sufficient room was left in the "seal area" to allow for testing a variety of seal configurations. Preliminary design had been accomplished on a previous program of a ring seal using mating surfaces coated or impregnated with MoS_2. While this still seemed a promising approach, reported experience with MoS_2 in the space environment is limited to use in bearings, and it appeared that fabrication of the seal using this material might require considerable development effort. Hence, while sufficient room was allowed in the dummy hub to permit later inclusion of an MoS_2 seal should that be desirable, it was decided first to check into possible gasket and O-ring-type seals.

In preliminary attempts at sealing the hub, O-ring seals were tried, but it was found impossible to maintain negligible leak rates without extremely high "squeeze" on the O-ring and thus very high friction levels for the hub.

Another solution attempted was the ring seal shown in Figure 15. This seal was made of a commercially available polyurethane compound, and it was not molded but actually machined out of a plate of the material. The plate was spun in a lathe with the axis of rotation normal to the plane of the plate. A small thin knife blade was fed into the polyurethane, cutting the washer. The washer was cut to have a 0.1 mm interference fit with the mating surface of the moving member of the hub.

After solving preliminary problems connected with sealing the test fixture itself, tests of the polyurethane seal were run by pressurizing the test fixture to one atmosphere gauge, and checking the starting and running torques in both directions of rotation after varying periods of rest. At first, starting torques were well outside the range of 0 - 50-inch-pound (0-5.65 meter-newton) torque wrench. The hub was then disassembled, and the sealing surface of the inner hub, which had been a smoothly machined anodized surface, was polished somewhat, using optical rouge. Upon reassembly, the highest starting torque was 5.6 meter-newtons in one direction and about 3.4 meter-newtons in the other. Running torque varied from 2.3 - 4.5 meter-newtons, depending on speed and direction of rotation. The marked difference in torque in the two directions seemed consistent. This was attributed to microscopic assymetries on the surface of the hub. Undoubtedly, the hub was machined with the tool running in one direction only, and the polishing operation, mentioned above, was also done in only one direction.

The next thing that was tried was a light application of tungsten diselenide to the inner surface of the hub. This substance is a fine black powder which very much resembles powdered graphite. According to

the manufacturer, however, its performance in a vacuum is markedly different from that of graphite. The lubrication properties of graphite are dependent on water trapped in the graphite structure. When this water evaporates the graphite looses its lubricity. The lubricity of the tungsten diselenide, on the other hand, is not dependent on foreign materials but is a characteristic of the compound itself. It is characterized by tenacious adhesion to anything it touches, particularly the fingers of the experimenter. The substance was applied to the inner diameter of the polyurethane ring and to the mating surface on the moving part of the hub. The seal was then re-assembled and the hub rotated for 1/2 hour at about 4 rpm. Thereafter, the fixture was pressurized to one atmosphere gauge and allowed to sit with the hub stationary for three days. At the end of that time starting torque was 2.3 meter-newtons in each direction, and after two revolutions in each direction starting and running torques were in the range of 1.1 - 2.0 meter-newtons.

At this point a leak test was run on the polyurethane seal under high-vacuum conditions. The test fixture was sealed at an internal pressure of one atmosphere absolute. The fixture was then put into a vacuum chamber and the vacuum pump started. The hub-drive motor was run continuously during the initial 17 hours of the testing to eliminate any pockets of air between the face of the seal and the mating face of the hub.

After this time, the motor was run for only 15 - 30 minutes per day to partially simulate the duty cycle that would be used within an orbiting reflectometer. Near the beginning of the test there was considerable outgassing, which limited the available vacuum to between 10^{-4} and 10^{-5} torr (1.3×10^{-2} and 1.3×10^{-3} newton/meter^2). This outgassing was attributed to a non-hardening sealant used around the pressurization valve of the seal test fixture. After three days in the test chamber, the outgassing apparently ceased and the chamber pressure decreased to 2.4×10^{-6} torr (3.3×10^{-4} newton/meter^2). After four days in the test chamber, the pump was turned off but the chamber was left sealed. The seal test fixture remained inside the vacuum chamber for an additional two days under vacuum conditions.

Following the test, starting and running torques were between 0.68 and 1.1 meter-newtons in both directions, measured with no pressure differential across the seal. While the test fixture was in the vacuum chamber, the vacuum level was monitored just before and just after starting the test fixture motor. If there had been any leak associated with hub motion we would expect the chamber pressure to increase sharply when the hub was started. No such pressure increase was noted. The test fixture temperature and the test fixture internal gauge pressure relative to the vacuum chamber were both monitored periodically during the test. The internal temperature increased to 41°C (105°F) during the initial period while the motor was running continuously. There was a

corresponding pressure rise during this period as well, attributable to heating of the air within the test fixture. With this exception, the pressure within the test fixture remained constant (to the modest accuracy of the test gauge used) for the period of the test.

To find an approximation for the maximum tolerable leak rate, we assume the simplest leakage situation, namely, that the leakage rate will be proportional to the pressure differential across the seal. This leads to an expression of the type

$$p(t) = P_o \exp(-t/T)$$

where

P_o = initial gage pressure
$p(t)$ = gage pressure at time t
T = the leakage "time constant", the time for the pressure to decrease to 63% of its initial pressure

If we assume the use of a dc motor within the reflectometer, the limiting factor will be sparking at the motor brushes. One motor manufacturer specifies that his brushes will operate at altitudes as high as 100 000 feet, (30.5 km) which corresponds to an ambient pressure of about 1.1×10^3 newton/meter^2. Thus, if we let $P_o = 10^5$ newton/meter^2, t = 365 days, and $p(t) = 1.1 \times 10^3$ newton/meter^2, then the leakage time constant would be about 80 days. In this case, the pressure after four days would be about 95% of the initial pressure. The indicated pressure in the test fixture increased 1.4×10^3 newton/meter^2 during the first three days of the vacuum chamber test. Even if we ascribe as large as a 3.5×10^3 newton/meter^2 error to meter repeatability and operator reading error, there was at most a 2% drop in internal pressure in the three-day period. Thus this seal, the first one tested, would amply meet the requirements imposed by the use of a dc motor inside the reflectometer. In the case that an ac motor were used, with its attendant dc to ac converter, the internal pressure necessary at the end of the mission would be considerably less, and the seal requirements correspondingly less stringent.

After the test fixture was removed from the vacuum chamber, it was decided to fabricate a second seal using a slightly different technique. The test hub was disassembled, the aluminum sealing surface of the moving member cleaned in methylethyl ketone and burnished with powdered tungsten diselenide. A polyurethane sealing ring was prepared by immersion for two minutes in an ultrasonic bath with methylethyl ketone, then dried and rubbed all over with the tungsten diselenide powder. The hub was then assembled using this seal, and run without pressurization for some 18 hours. It was then disassembled, recoated with additional tungsten diselenide powder, reassembled, and pressurized to 15 psi (10^5 newton/meter^2) gauge. After about 3-1/2 hours of continuous motor operation

at 4 rpm, the seal began to chatter and the motor speed decreased. Depressurization and disassembly showed the I.D. of the ring to be partially bare of tungsten diselenide, and somewhat galled.

The tungsten diselenide powder used had been of 40μ grain size. On the advice of the manufacturer of the powder, some 1 - 2μ grain sized tungsten diselenide was procured, and used to coat the same sealing ring that had been used in the successful vacuum chamber test. After assembly and pressurization, the drive motor was started, but the seal soon showed a high leak rate as well as the chattering and high friction level which had been characteristic of the previous failure.

It is evident that further work is necessary in the area of the rotating seal. A possible cause for the successful operation of the first polyurethane seal in the vacuum chamber test was that a silicone grease had been used in the assembly of the hub, and sufficient of this may have remained on the aluminum mating surface to prevent the galling which troubled the later tests. It should be noted, however, that the silicone lubricant used is one designed for space environment, and one which probably would be satisfactory for use again with an orbiting reflectometer.

Bearing Lubrication

A one-week vacuum weight-loss test was run on several lubricants which appeared promising for use in the bearing area of the hub assembly. Results are summarized in Table VII. This test was run with the lubricants in a vacuum chamber at less than 4×10^{-3} newton/meter^2 and temperatures ranging from 59°C to 107°C. Both of the oil samples showed some bubbling during the test; however, the bubbling of sample No. 2 occurred at the very start of the test and is attributed by the test technician to small air bubbles trapped during pouring. Bubbling of sample No. 5, however, continued throughout the test. This sample also showed some discoloration. While samples 3 and 4 showed less weight loss than sample 2, the latter was used to impregnate the bearings because of its low friction and ease of application.

TABLE VII

LUBRICANT VACUUM TEST RESULTS

Sample No.	Material	% Weight Change
1	Grease	-1.30
2	Oil	-0.31
3	Grease	-0.07
4	Grease (as sample 4)	-0.03
5	Oil	-0.03

The bearings to be used in the test hub were prepared by cleaning first in hectane solvent, then removing the solvent by heating to 118°C for 12 hours in a 1.3×10^{-4} newton/meter^2 vacuum. Bearings were then removed from the vacuum chamber, immediately immersed in the oil, and returned to the vacuum chamber and heated while the chamber was brought down to a vacuum of 1.3×10^{-2} newton/meter^2. This treatment effectively backfilled the phenolic bearing retainers.

Seal Weight Loss Test

Four different samples of the polyurethane material which had been used for seals were subjected to nine-day weight loss tests in a vacuum chamber. Pressure in the vacuum chamber was maintained at less than 1.3×10^{-2} newton/meter^2 throughout the test. Samples were weighed before and after the test and the differences noted. Average sample weight was about 10 grams, and while the samples were scraps of material, and thus had varying shapes, each was about 2.5-mm thick and a surface area (for one side) of approximately 50 cm^2. Weight loss for the nine-day period ranged from 0.48% - 0.62%.

It is felt that this very modest weight loss indicates that this material might well be suitable for space applications.

CONCLUSIONS AND RECOMMENDATIONS

This program has advanced the state of the art of reflectometer instrumentation to a point where flight qualification development can, and should, be initiated. High output solar power systems will be urgently needed in the very near future for a variety of space missions.

The feasibility of reflective solar concentrators depends most critically on a flight demonstration to show that the reflectance can be maintained at a high level throughout the system design lifetime. It is essential that representative samples of solar concentrator surface materials be subjected to a long-term orbital flight test to prove the durability of the surfaces under solar ultraviolet radiation, micrometeorites, and low energy protons.

The optical layout of the reflectometer can be folded in a variety of ways, depending on the envelope size and shape available in the satellite. Thus, choice of satellite must be made before this design is begun. Design of a flightworthy instrument should include careful analysis of the dynamic torques produced by the moving arm. If necessary, a contra-rotating member can be built into the reflectometer itself, although at some penalty in weight.

Additional effort is required to resolve the dependence of indicated reflectance on sample geometry. One solution is to measure the temperature of each sample during flight, and to correct the observed reflectance readings with temperature-curvature curves previously prepared on earth. Samples should be mounted in stress-free mounts, to preclude sample geometry changes from causes other than temperature. In any event, temperature of each sample should be measured in flight as general backup information.

Another design effort involves seal fabrication and testing. Optimal seal design parameters should be determined by fabricating and testing a number of seals. Further, the polyurethane material used for the seal should be tested and evaluated more intensively than was possible on the present program. In particular, it should be determined whether any outgassing products produced are of such as to coat nearby optics, or whether they are simply harmless substances such as surface-absorbed water.

REFERENCES

1. Computed from tables in "Index of Refraction of Fused Quartz Glass for Ultraviolet, Visible, and Infrared Wavelengths," Rodney and Spindler, JOSA 44 (1954), and letter from T. L. Van Raalte, JOSA, 50 (1960)

2. Parcel, R. W., F. J. Clause, C. F. O'Hara, and W. C. Young, in 1963 Transactions of Tenth National Vacuum Symposium, American Vacuum Society, MacMillan Co., New York, 1963 (abstracted from "Lubrication and Wear in Space Systems")

LIBRARY ABSTRACT CARD

NASA CR-66010

Prepared under NAS1-4660 by Electro-Optical Systems, Inc., Pasadena, California

Development of a Second Generation Prototype Reflectometer for Reflectance Measurement in Space.

A second generation prototype reflectometer was developed and tested. This unit will be used to measure the reflectance of various samples under laboratory conditions. Various tests are described using sun image and vacuum ambient. Seals and lubricants were evaluated.

Arthur A. Olsen
Peter A. Button
D. H. McClelland

NASA CR-66010